

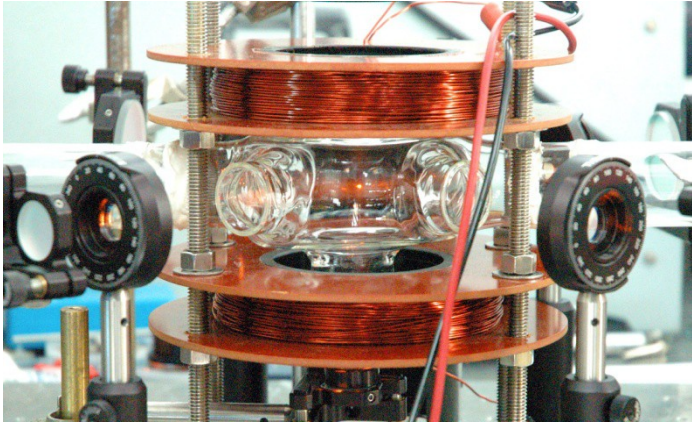
Vortices and other topological defects in ultracold atomic gases

Michikazu Kobayashi (Kyoto Univ.)

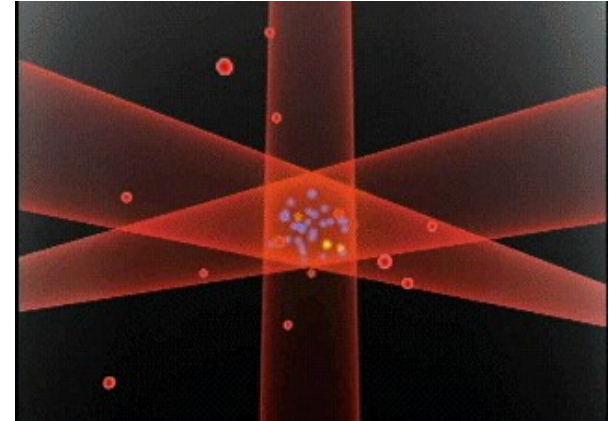
1. Introduction of topological defects in ultracold atoms
2. Kosterlitz-Thouless transition in spinor Bose gases
3. Non-abelian vortices

Feb. 21, 2016 “ χ -Mag 2016 Symposium”

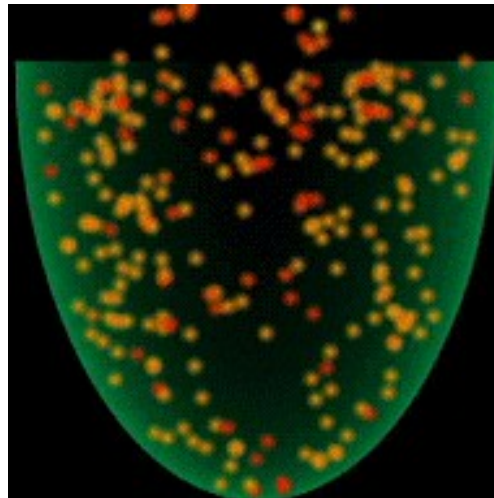
Ultracold atomic gases



Trapping atoms



Laser cooling : $\sim\mu\text{K}$



Evaporative cooling :
 $\sim\text{nK}$

Ultracold atomic gases

hydrogen 1 H 1.0079																	helium 2 He 4.0026						
lithium 3 Li 6.941	beryllium 4 Be 9.0122																	boron 5 B 10.811	carbon 6 C 12.011	nitrogen 7 N 14.007	oxygen 8 O 15.999	fluorine 9 F 18.998	neon 10 Ne 20.180
sodium 11 Na 22.990	magnesium 12 Mg 24.305																	aluminium 13 Al 26.982	silicon 14 Si 28.086	phosphorus 15 P 30.974	sulfur 16 S 32.065	chlorine 17 Cl 35.453	argon 18 Ar 39.948
potassium 19 K 39.098	calcium 20 Ca 40.078	scandium 21 Sc 44.956	titanium 22 Ti 47.867	vanadium 23 V 50.942	chromium 24 Cr 51.996	manganese 25 Mn 54.938	iron 26 Fe 55.845	cobalt 27 Co 58.933	nickel 28 Ni 58.693	copper 29 Cu 63.546	zinc 30 Zn 65.39	gallium 31 Ga 69.723	germanium 32 Ge 72.61	arsenic 33 As 74.922	selenium 34 Se 78.96	bromine 35 Br 79.904	krypton 36 Kr 83.80						
rubidium 37 Rb 85.468	strontium 38 Sr 87.62	yttrium 39 Y 88.906	zirconium 40 Zr 91.224	niobium 41 Nb 92.906	molybdenum 42 Mo 95.94	technetium 43 Tc [98]	ruthenium 44 Ru 101.07	rhodium 45 Rh 102.91	palladium 46 Pd 106.42	silver 47 Ag 107.87	cadmium 48 Cd 112.41	indium 49 In 114.82	tin 50 Sn 118.71	antimony 51 Sb 121.76	tellurium 52 Te 127.60	iodine 53 I 126.90	xenon 54 Xe 131.29						
caesium 55 Cs 132.91	barium 56 Ba 137.33	57-70 *	lutetium 71 Lu 174.97	hafnium 72 Hf 178.49	tantalum 73 Ta 180.95	tungsten 74 W 183.84	rhenium 75 Re 186.21	osmium 76 Os 190.23	iridium 77 Ir 192.22	platinum 78 Pt 195.08	gold 79 Au 196.97	mercury 80 Hg 200.59	thallium 81 Tl 204.38	lead 82 Pb 207.2	bismuth 83 Bi 208.98	polonium 84 Po [209]	astatine 85 At [210]	radon 86 Rn [222]					
francium 87 Fr [223]	radium 88 Ra [226]	89-102 **	lanthanum 103 La [227]	rutherfordium 104 Rf [261]	dubnium 105 Db [262]	seaborgium 106 Sg [266]	bohrium 107 Bh [264]	hassium 108 Hs [269]	meitnerium 109 Mt [268]	ununnium 110 Uun [271]	ununium 111 Uuu [272]	ununium 112 Uub [277]	ununquadium 114 Uuq [289]										

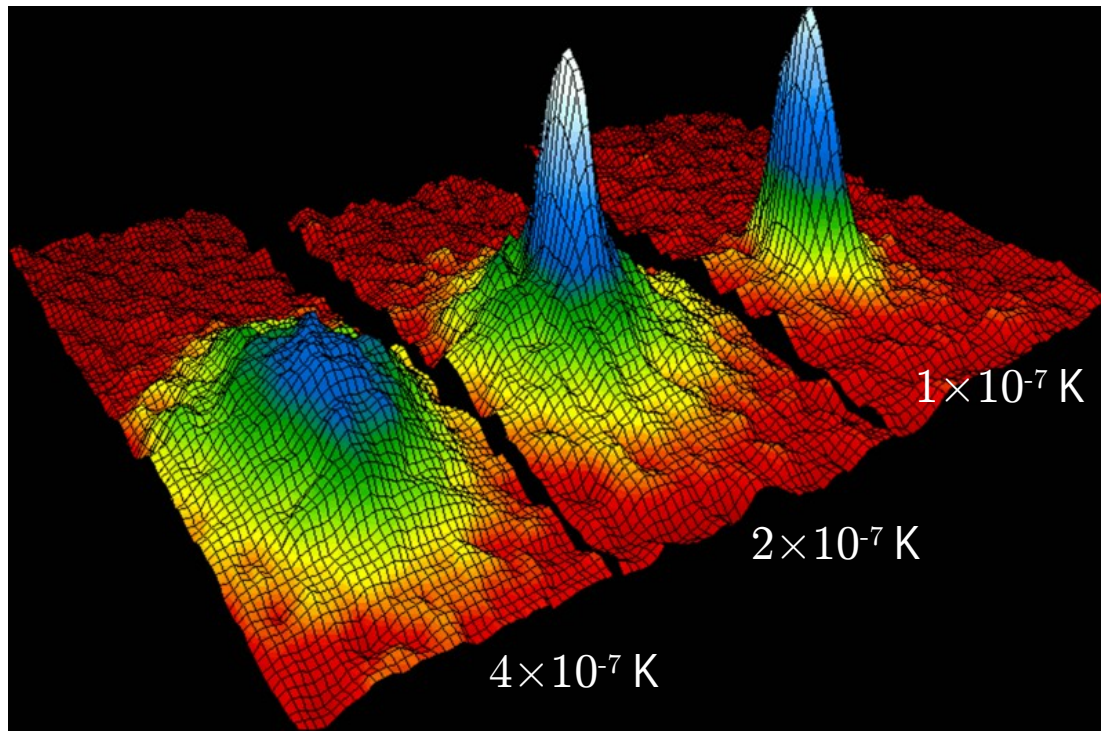
* Lanthanide series

lanthanum 57 La 138.91	cerium 58 Ce 140.12	praseodymium 59 Pr 140.91	neodymium 60 Nd 144.24	promethium 61 Pm [145]	samarium 62 Sm 150.36	europium 63 Eu 151.96	gadolinium 64 Gd 157.25	terbium 65 Tb 158.93	dysprosium 66 Dy 162.50	holmium 67 Ho 164.93	erbium 68 Er 167.26	thulium 69 Tm 168.93	ytterbium 70 Yb 173.04
actinium 89 Ac [227]	thorium 90 Th 232.04	protactinium 91 Pa 231.04	uranium 92 U 238.03	neptunium 93 Np [237]	plutonium 94 Pu [244]	americium 95 Am [243]	curium 96 Cm [247]	berkelium 97 Bk [247]	californium 98 Cf [251]	einsteinium 99 Es [252]	fermium 100 Fm [257]	mendelevium 101 Md [258]	nobelium 102 No [259]

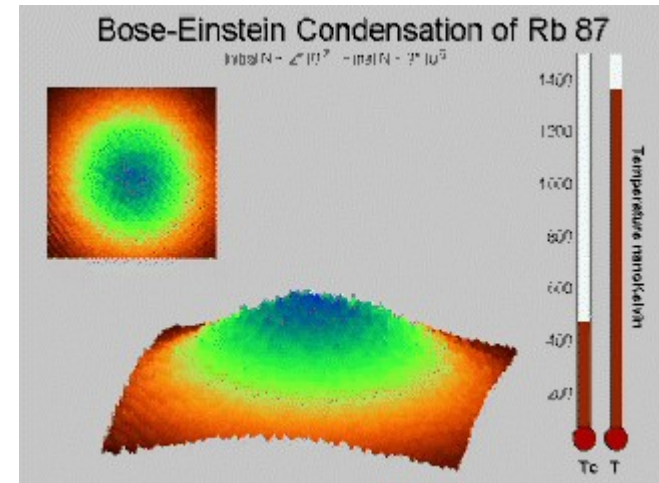
** Actinide series

Bose-Einstein condensation

Experimental image for momentum distribution of Bose atoms (^{87}Rb)



Temperature and condensation



JILA, 1995

Similar images are obtained for cooper pairs and bounded pairs (molecules) of Fermi atoms

Comparison with condensed matter systems (electrons and superfluid helium)

	condensed matter	cold atoms
density (m^{-3})	10^{28-31} (dense)	10^{16-23} (dilute)
uniformity	uniform	not uniform (trapped)
microscopic dynamics	ps - ns (rapid)	μs - ms (slow)
conservation	open system	isolated system

- Perturbation theory is valid for quantitative comparison between microscopic theories and experiments
- Interaction strength is also controllable

Order parameter

Bosons

$\langle \psi^\dagger(x)\psi(x') \rangle \xrightarrow{|x-x'|} \psi^*(x)\psi(x') : \text{Bose-Einstein condensation}$

Fermions

$\langle \psi_\sigma^\dagger(x)\psi_{\sigma'}^\dagger(x)\psi_{\sigma'}(x')\psi_\sigma(x') \rangle \xrightarrow{|x-x'|} \Delta^*(x)\Delta(x') : \text{Cooper pairing}$

$\psi(x) = |\psi(x)|e^{i\phi(x)} : \text{spontaneous symmetry breaking}$
for $U(1)$ -phase shift

$\rho(x) = |\psi(x)|^2 : \text{particle density}$

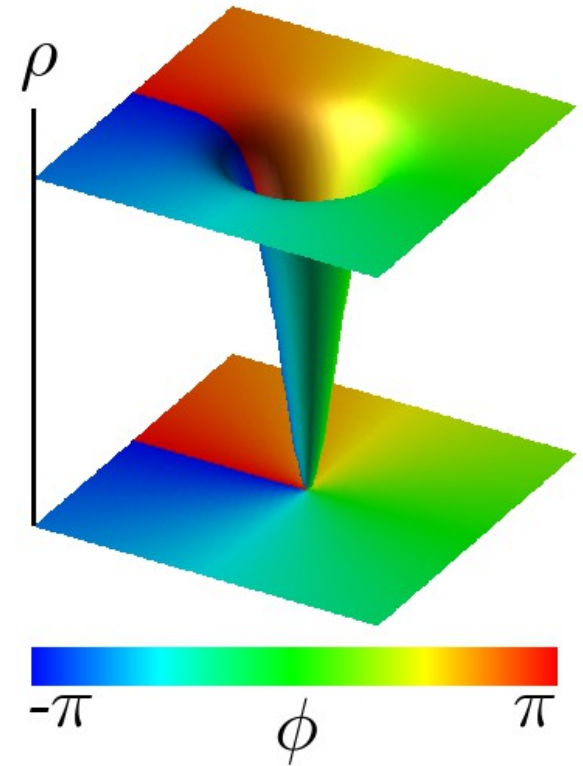
$\mathbf{v}(x) = \frac{\hbar}{M} \nabla \phi(x) : \text{superfluid velocity}$

Quantized vortex

$$\psi(x) = |\psi(x)|e^{i\phi(x)}$$

$$\rho(x) = |\psi(x)|^2 : \text{particle density}$$

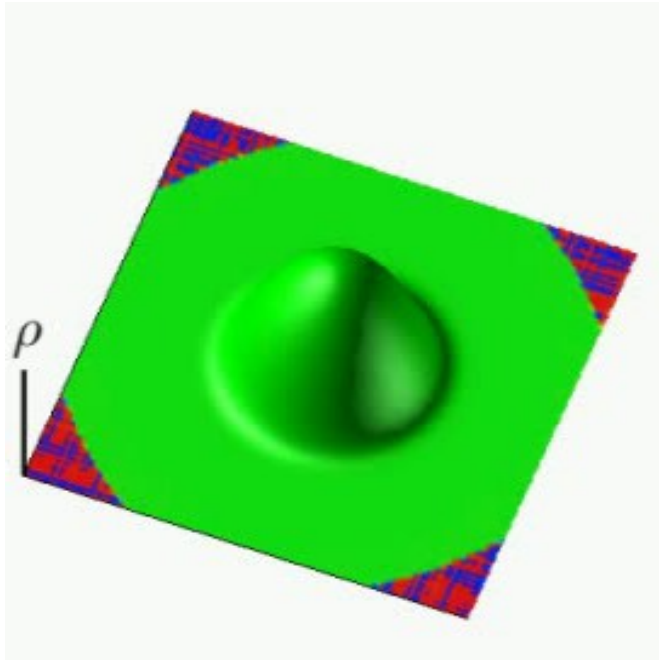
$$\mathbf{v}(x) = \frac{\hbar}{M} \nabla \phi(x) : \text{superfluid velocity}$$



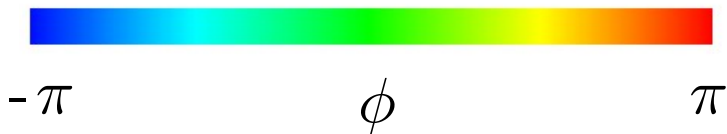
Vortex appears as topological defect for $U(1)$ phase shift
(density $\rho(x)$ vanishes)

Vortex lattice formation

Simulation of the non-linear Schrödinger equation

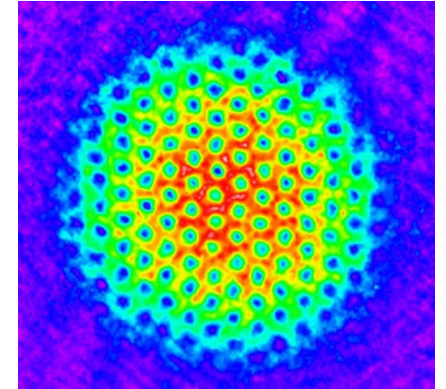
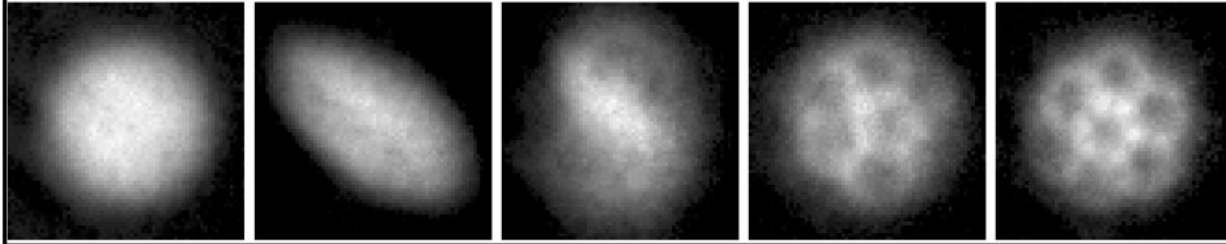


- Phase vortices appear in the outside of the condensate
- Condensate is squashed
- Vortices excite the surface of the condensate
- Vortices enter the condensate
- Triangular vortex lattice is formed



Vortex lattice formation

Vortex lattice in ^{87}Rb BEC

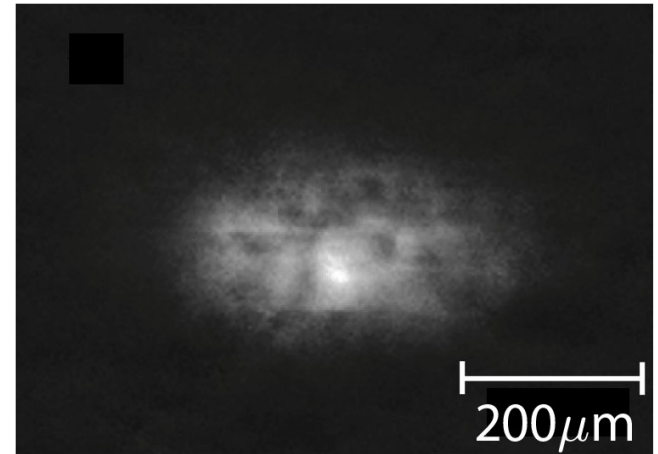
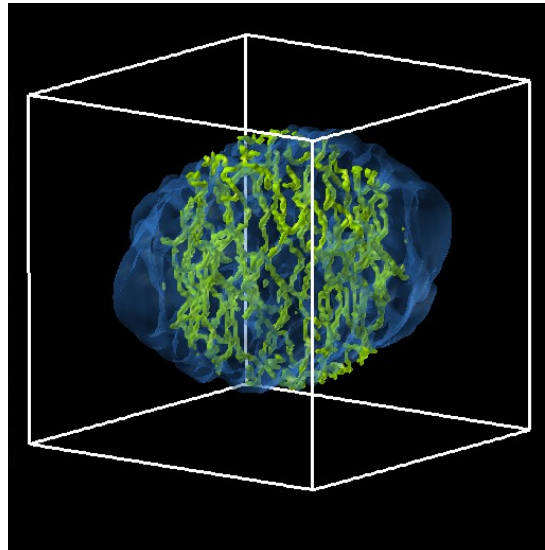
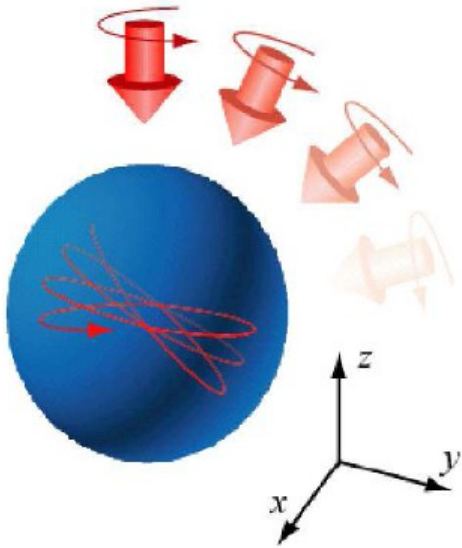


K. W. Madison et al. PRL **86**, 4443 (2001)

Quantum turbulence

Precession rotation of condensation

PRA **76**, 045603 (2007)



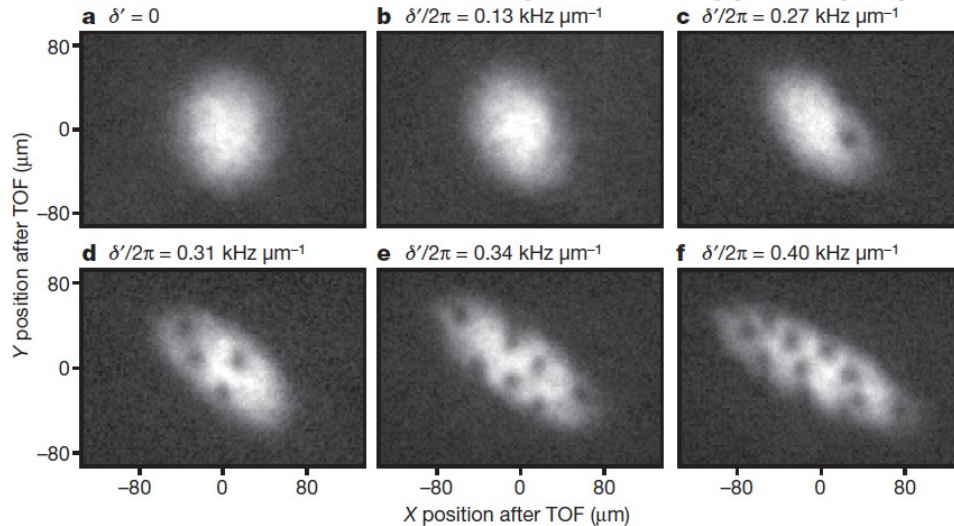
PRL **103**, 045301 (2009)

Vortices are not lattice but tangled (quantum turbulence)

Other method to excite vortices

Artificial magnetic (gauge) field

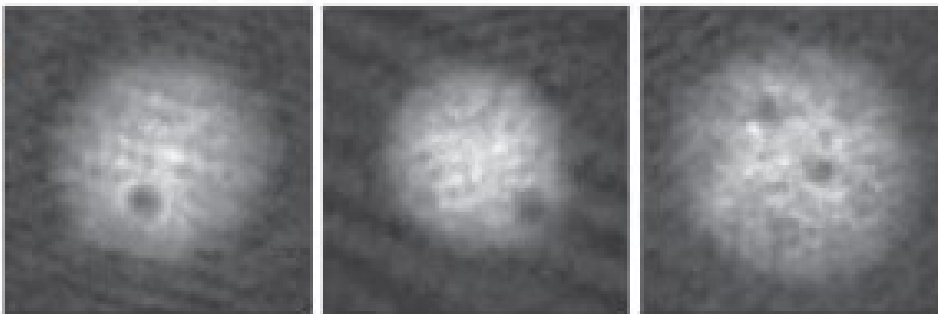
Nature **462**, 628 (2009)



No centrifugal force
→ Large number of vortices can be excited
→ Toward quantum Hall state

rapid temperature quench

Nature **455**, 948 (2008)



- Phase imprinting
- Interaction with Laguerre-Gaussian beam

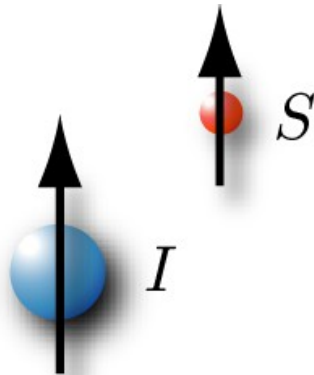
Internal degrees of freedom

- Multi-component condensate
- Spinor condensate

type of particle trap	spin degrees of freedom	type of condensate
magnetic trap	frozed	scalar condensate
optical trap	alived	spinor condensate

Hyperfine coupling of nuclear and electron spins :

$$F = I \text{ (nuclear spin)} + S \text{ (electron spin)} + L \text{ (electron orbital)}$$

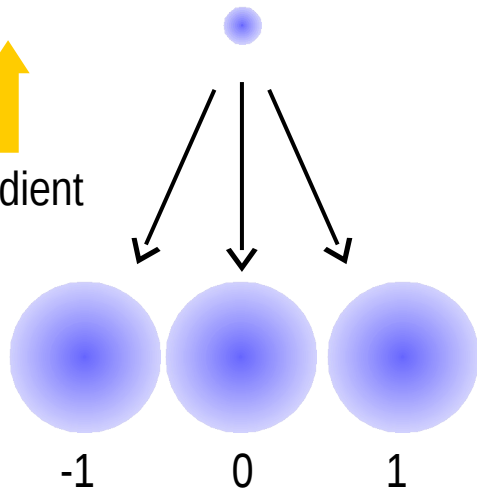


$^{87}\text{Rb}, ^{23}\text{Na}$ $^7\text{Li}, ^{41}\text{K}$	$F = 1, 2$
^{85}Rb	$F = 2, 3$
^{133}Cs	$F = 3, 4$
^{52}Cr	$S = 3, I = 0$

Spinor condensate

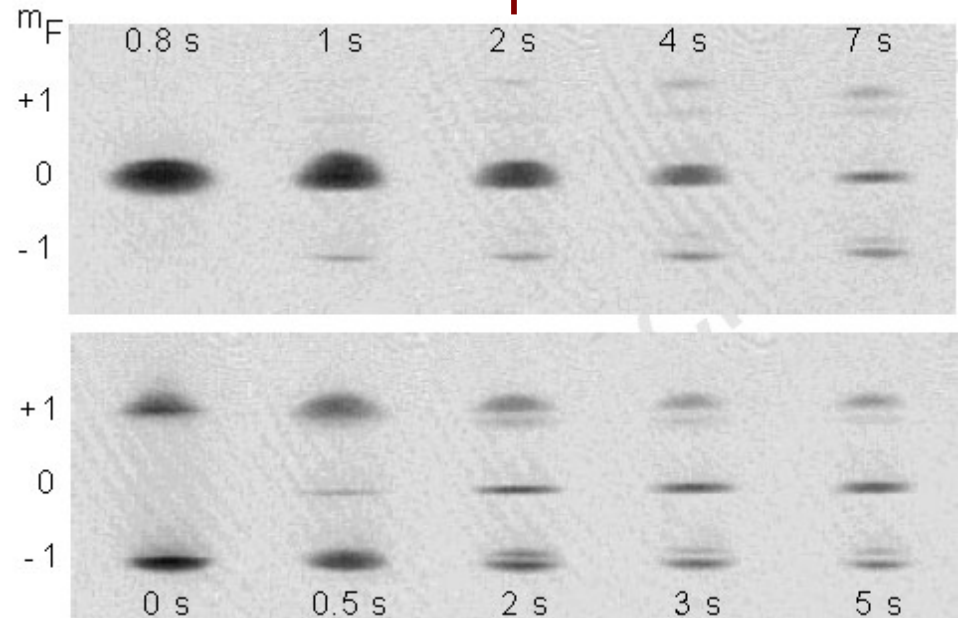
$$^{87}\text{Rb} (I = 3/2, S = 1/2, L = 0) \rightarrow F = 1, 2$$

Field gradient



Stern-Gerlach experiment

$F = 1$ experiment



J. Stenger et al. Nature **396**, 345 (1998)

Mean-field theory for spinor condensates

order parameter : $\psi = (\psi_F \quad \psi_{F-1} \quad \cdots \quad \psi_{-F})$

$$\text{spin-1 : } H = H_0 + \frac{2\pi\hbar^2}{M} \int d\mathbf{x} (a_0\rho^2 + a_1\mathbf{S}^2)$$

$$\text{spin-2 : } H = H_0 + \frac{2\pi\hbar^2}{M} \int d\mathbf{x} (a_0\rho^2 + a_1\mathbf{S}^2 + a_2|A_{20}|^2)$$

1-body part

$$H_0 = \int d\mathbf{x} \left[\sum_{m=-F}^F \left\{ \frac{\hbar^2}{2M} |\nabla\psi_m|^2 + (q_1 m + q_2 m^2 + V) |\psi_m|^2 \right\} \right]$$

q_1 : linear-Zeeman coefficient

q_2 : quadratic-Zeeman coefficient

V : 1-body external trapping potential

Mean-field theory for spinor condensates

order parameter : $\psi = (\psi_F \quad \psi_{F-1} \quad \cdots \quad \psi_{-F})$

$$\text{spin-1 : } H = H_0 + \frac{2\pi\hbar^2}{M} \int d\mathbf{x} (a_0\rho^2 + a_1\mathbf{S}^2)$$

$$\text{spin-2 : } H = H_0 + \frac{2\pi\hbar^2}{M} \int d\mathbf{x} (a_0\rho^2 + a_1\mathbf{S}^2 + a_2|A_{20}|^2)$$

$a_{0,1,2}$: s -wave scattering length

$\rho = \psi^\dagger\psi$: density

$\mathbf{S} = \psi^\dagger\hat{\mathbf{S}}\psi$: spin density

$A_{20} = \sum_{m=-F}^F (-1)^m \psi_m \psi_{-m}$: singlet-pair amplitude
(expectation value of unitary operator)

Ground states for spin-1 condensates without Zeeman field

$$H = \int d\mathbf{x} \sum_{m=-1}^1 \left(\frac{\hbar^2}{2M} |\nabla \psi_m|^2 + V |\psi_m|^2 \right) + \frac{1}{2} (g_0 \rho^2 + g_1 \mathbf{S}^2)$$

$$g_{0,1,2} = \frac{4\pi \hbar^2 a_{0,1,2}}{M}$$

$g_1 > 0$: polar (^{23}Na BEC)

$$e^{i\phi} e^{-i\mathbf{n} \cdot \hat{\mathbf{S}} \alpha} \begin{pmatrix} 0 \\ 1 \\ 0 \end{pmatrix}$$

$$|\mathbf{S}| = 0$$

$g_1 < 0$: Ferromagnetic (^{87}Rb BEC)

$$e^{i\phi} e^{-i\mathbf{n} \cdot \hat{\mathbf{S}} \alpha} \begin{pmatrix} 1 \\ 0 \\ 0 \end{pmatrix}$$

$$|\mathbf{S}| = 1$$

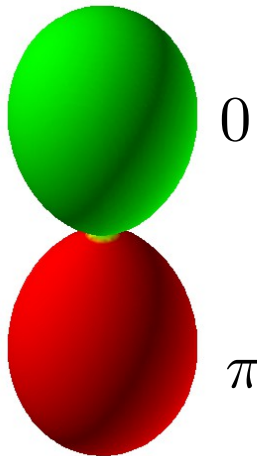
Representation with spherical-harmonic function

$$\sum_{m=-1}^1 \psi_m Y_{1,m} = Y_{1,1} + Y_{1,0} + Y_{1,-1}$$

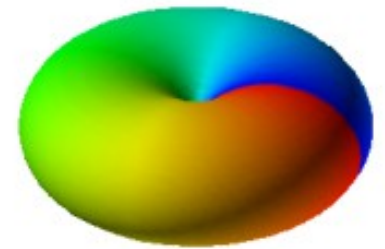
$\cos \theta$

$-e^{i\varphi} \sin \theta$

Polar
(dumbbell)

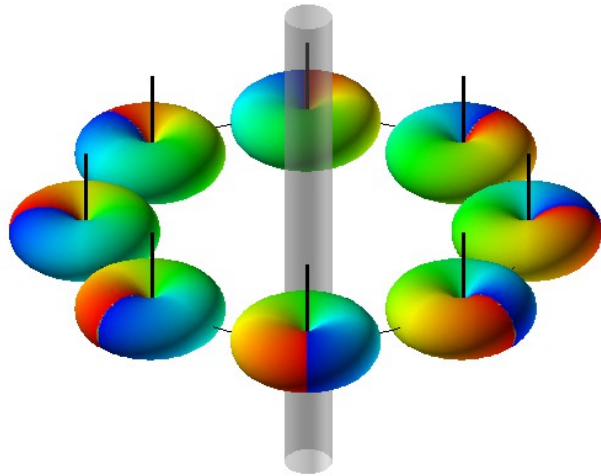


Ferromagnetic
(torus)



Vortex in Ferromagnetic phase

Phase vortex

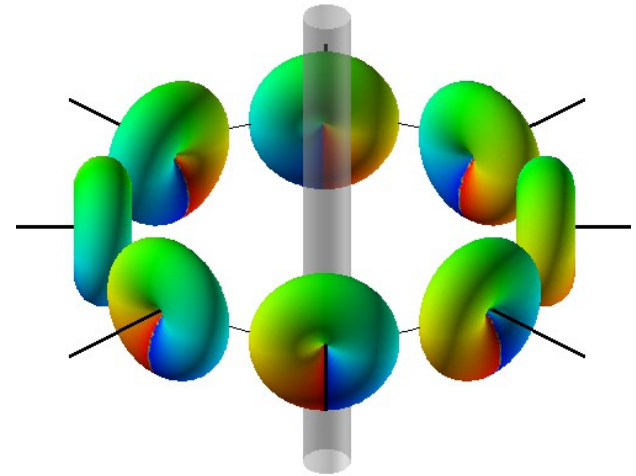


$$\psi = \begin{pmatrix} e^{i\phi} \\ 0 \\ 0 \end{pmatrix}$$

Continuously transformed



Spin vortex

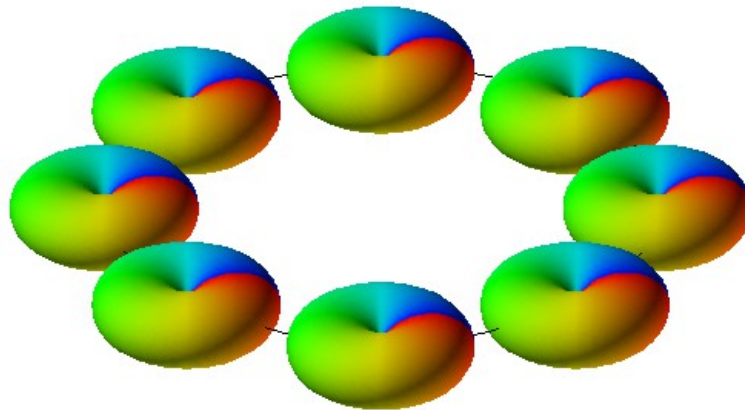


$$\psi = \frac{1}{2} \begin{pmatrix} 1 \\ \sqrt{2}e^{i\phi} \\ 1 \end{pmatrix}$$

Vortex in Ferromagnetic phase

Double winding vortex is continuously transformed to uniform state (phase imprinting)

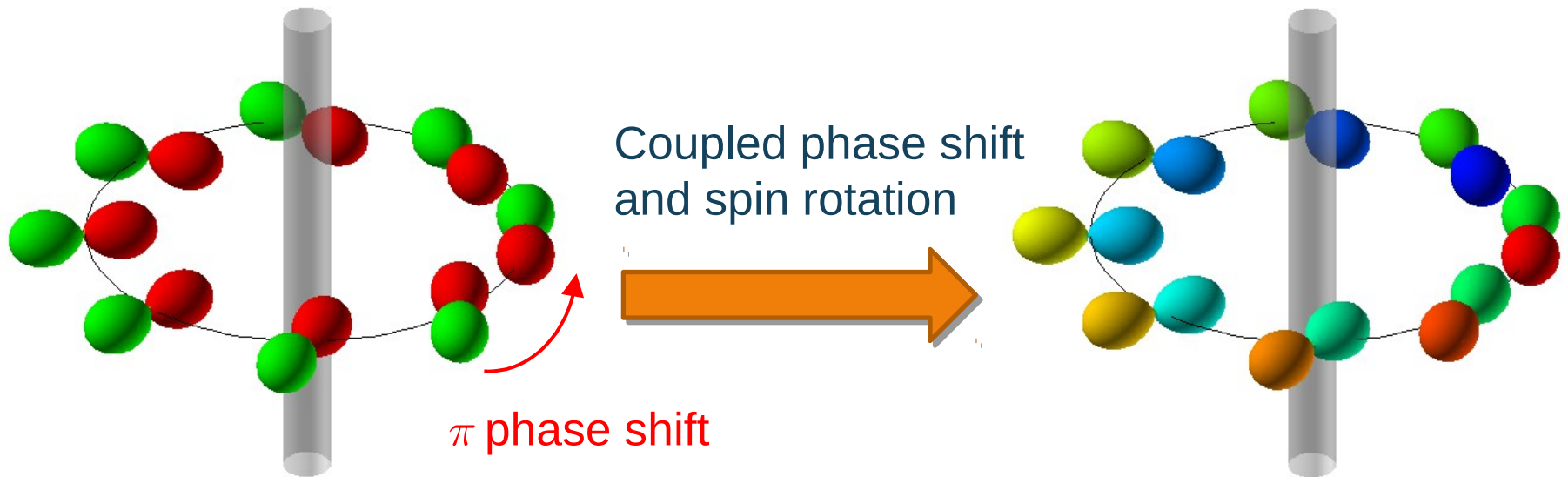
→ \mathbb{Z}_2 vortex



PRA **89**, 190403 (2002)

PRL **93**, 160406 (2004)

Vortex in polar phase

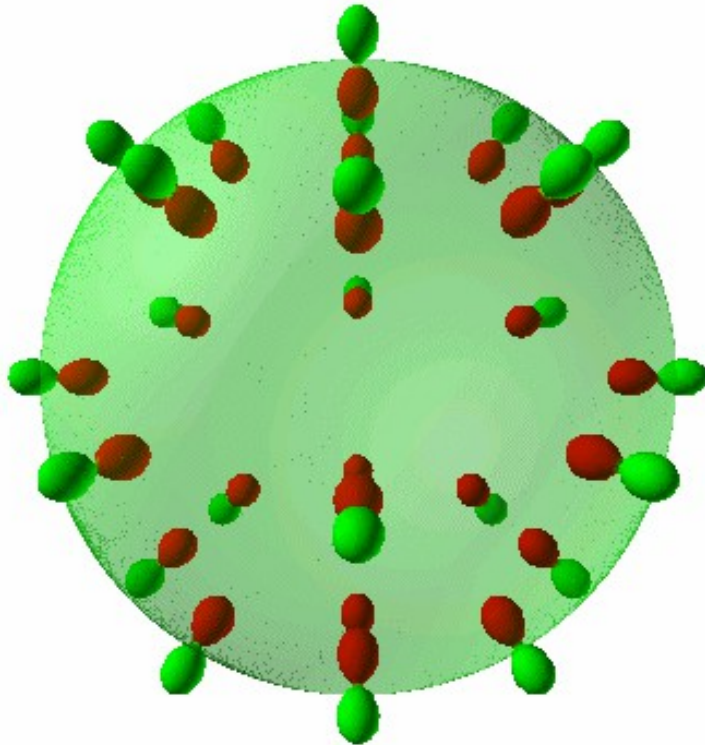


$$\psi = \frac{1}{\sqrt{2}} \begin{pmatrix} -e^{i\phi} \\ 0 \\ 1 \end{pmatrix}$$

Mass circulation around the vortex is half of that of scalar condensate (half-quantized vortex)

Monopole in polar phase

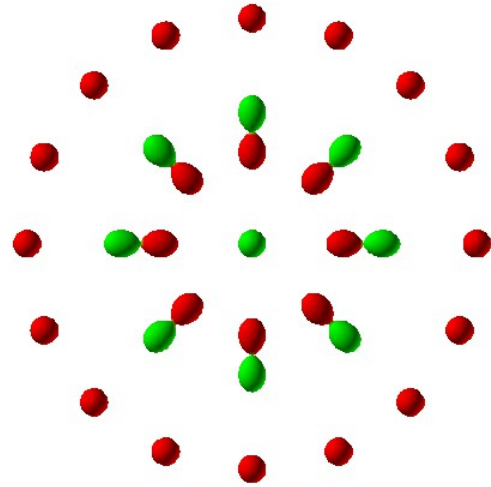
't Hooft-Polyakov monopole
in Polar phase



$$\psi = \frac{1}{\sqrt{2}} \begin{pmatrix} -e^{-i\phi} \sin \theta \\ \cos \theta \\ e^{i\phi} \sin \theta \end{pmatrix}$$

Monopole cannot exist in
Ferromagnetic phase

2D skyrmion in polar phase



$$\psi = \frac{1}{\sqrt{2}} \begin{pmatrix} -e^{-i\phi} \sin f(r) \\ \cos f(r) \\ e^{i\phi} \sin f(r) \end{pmatrix}$$

$$f(0) = 0 \quad f(r \rightarrow \infty) = \pi$$

Experimentally created by Laguerre-Gaussian beam

ψ_1

ψ_0

ψ_{-1}

Vortex-skyrmion
combined state
(metastable)

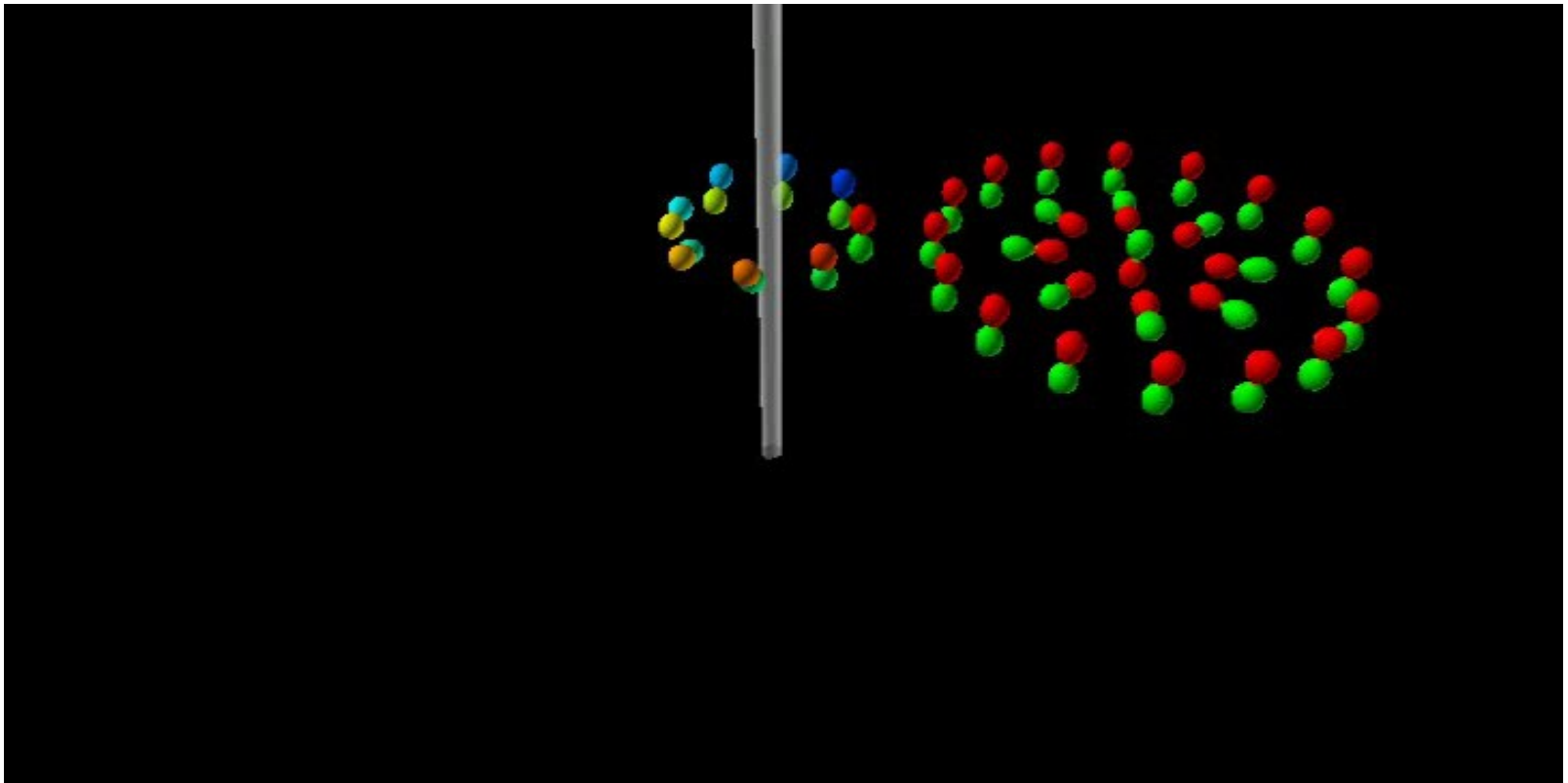


Phys. Rev. Lett. **103** 50401, (2009)

$$\psi = \frac{1}{\sqrt{2}} \begin{pmatrix} -e^{-2i\phi} \sin f(r) \\ e^{-i\phi} \cos f(r) \\ \sin f(r) \end{pmatrix}$$

Interaction between 2D skyrmion and half-quantized vortex

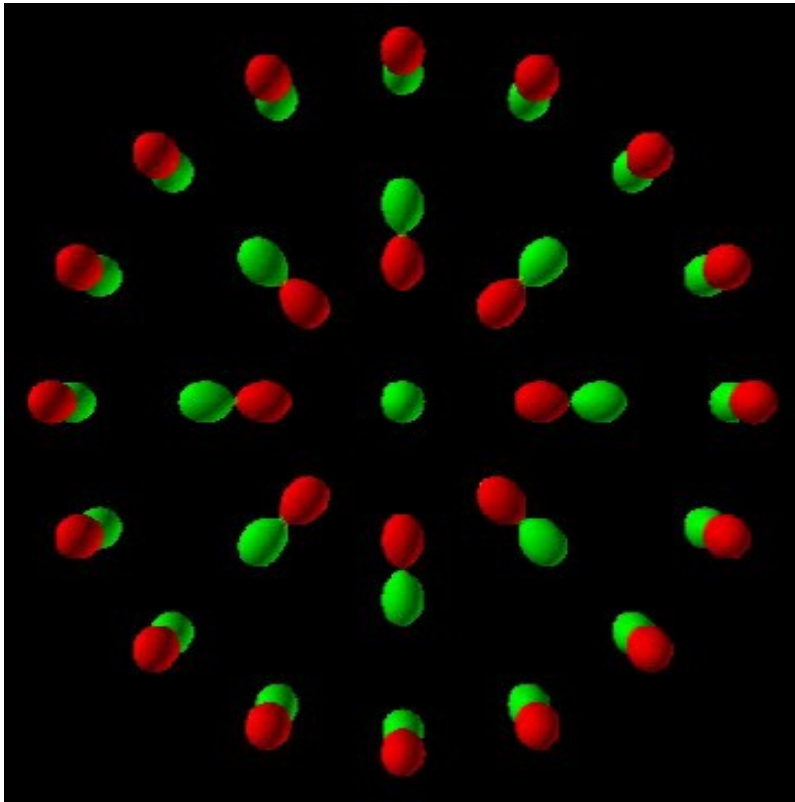
Skyrmion rotates around the half-quantized vortex



S. Kobayashi, et al. Nucl. Phys. B **856**, 577 (2012)

Interaction between 2D skyrmion and half-quantized vortex

Skyrmion rotates around the half-quantized vortex



Skyrmion charge is inverted when skyrmion rotates around the half-quantized vortex

→ \mathbb{Z}_2 skyrmion

S. Kobayashi, et al. Nucl. Phys. B **856**, 577 (2012)

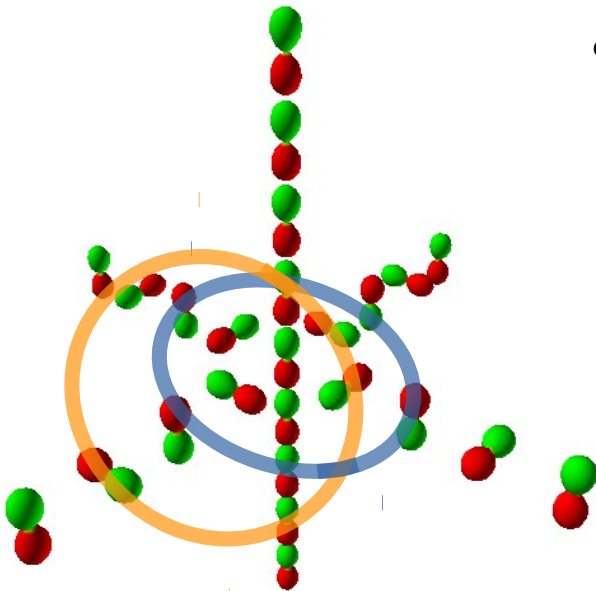
Short summary

Spinor condensates induce a variety of topological defects

	π_1	π_2	π_3
Polar	half-quantized vortex	monopole 2D \mathbb{Z}_2 skyrmion	Hopfion
Ferro	\mathbb{Z}_2 vortex		3D skyrmion

Hopfion

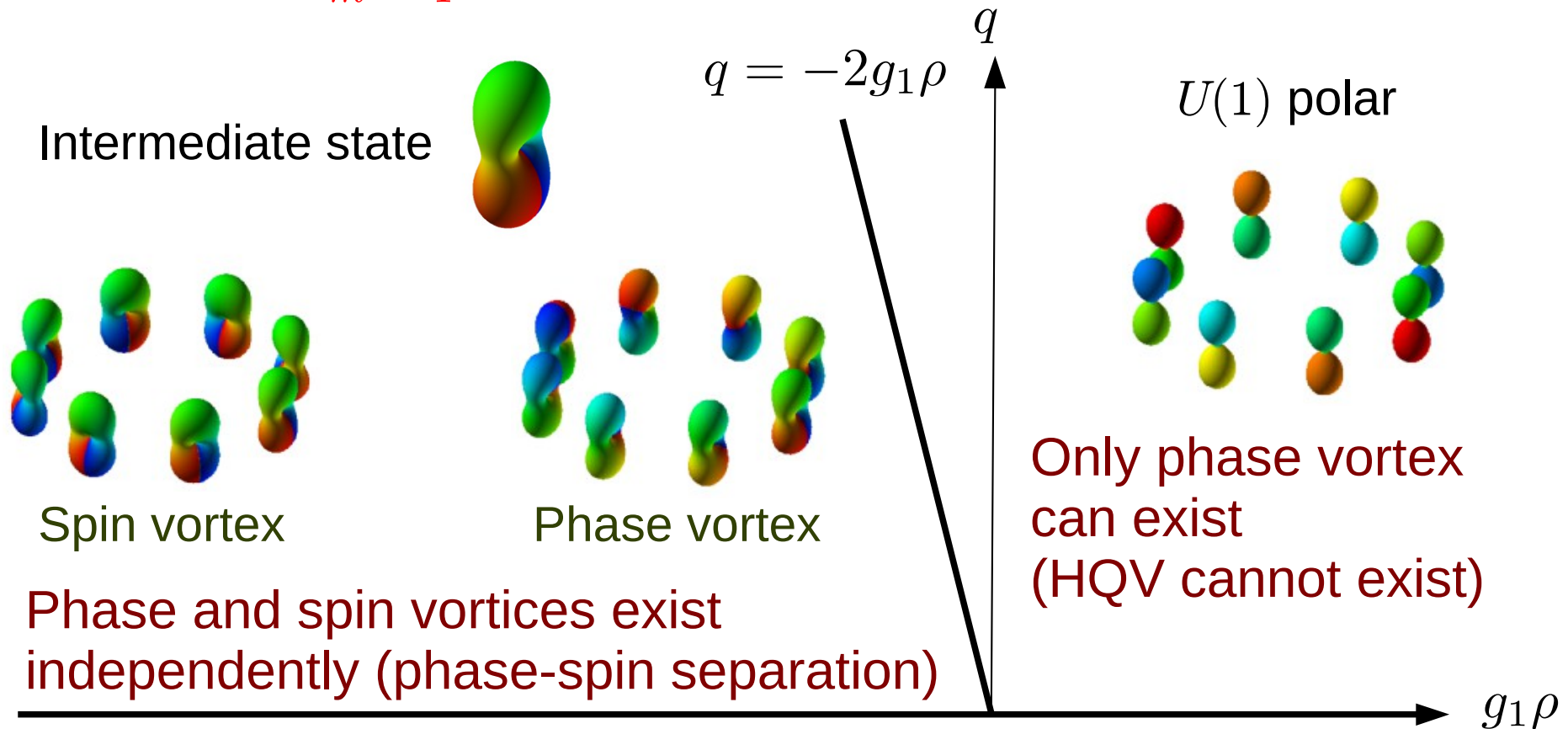
- Orbit of the same spin state has 1D ring
- Arbitrary 2 rings form the Hopf link



Phys. Rev. Lett. **100** 180403, (2008)

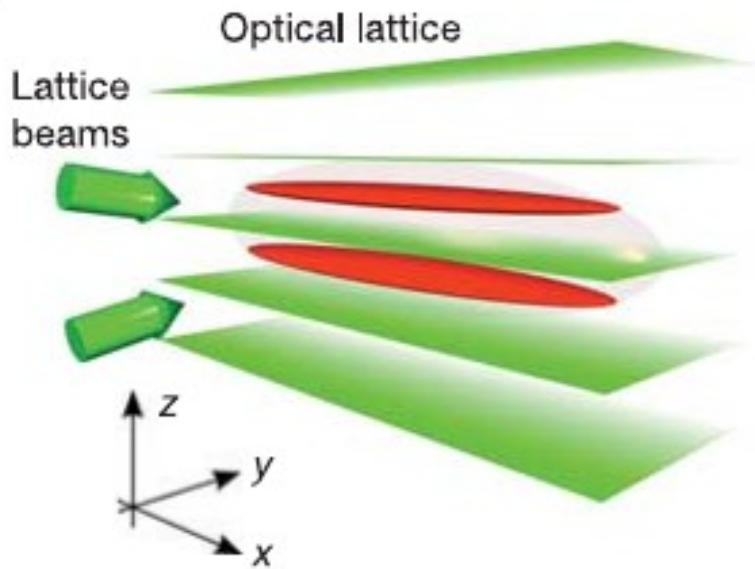
Spin-1 condensates under quadratic Zeeman field

$$H = \int d\mathbf{x} \sum_{m=-1}^1 \left(\frac{\hbar^2}{2M} |\nabla \psi_m|^2 + q_2 m^2 |\psi_m|^2 \right) + \frac{1}{2} (g_0 \rho^2 + g_1 \mathbf{S}^2)$$



Kosterlitz-Thouless transition in 2D system

Relationship between properties of vortex and KT transition?



2D system can be created by using optical standing wave

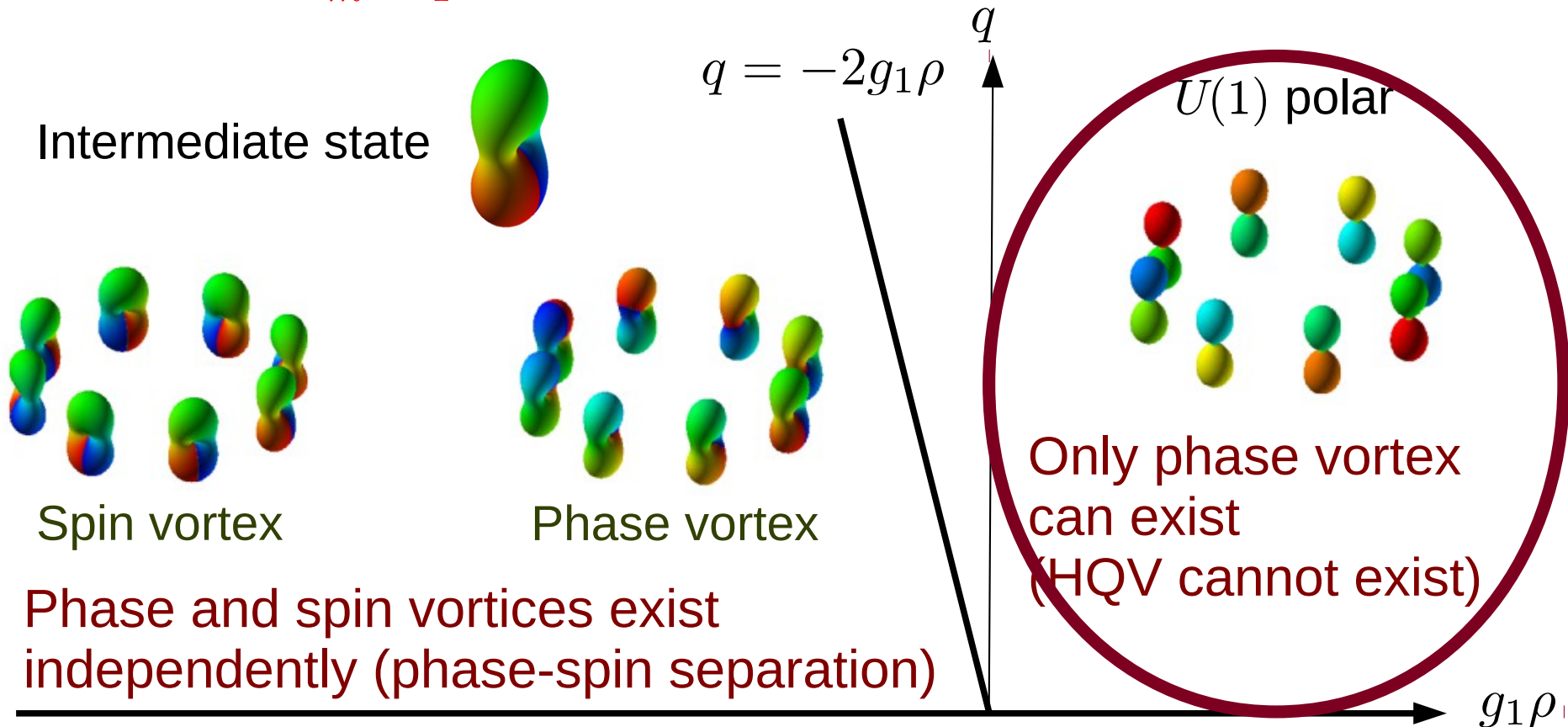
Monte-Carlo simulation

$$\langle f \rangle = \left(\prod_{m=-1}^1 \int D\psi_m D\psi_m^* \right) \times f[\psi_m, \psi_m^*] e^{-H/T}$$

Important value :
helicity modules for phase shift and spin rotation

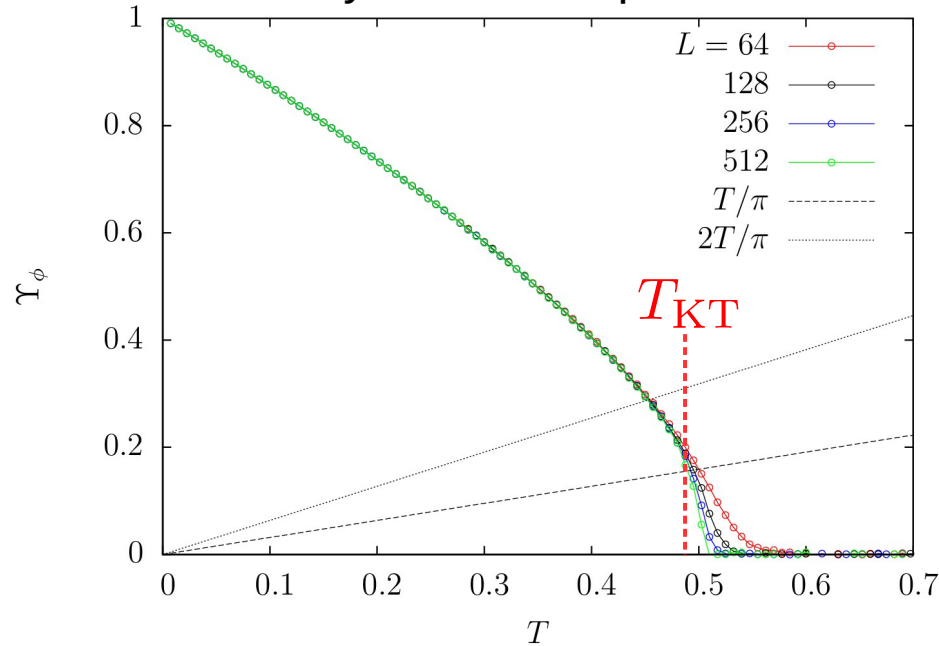
Kosterlitz-Thouless transition in 2D system

$$H = \int d\mathbf{x} \sum_{m=-1}^1 \left(\frac{\hbar^2}{2M} |\nabla \psi_m|^2 + q_2 m^2 |\psi_m|^2 \right) + \frac{1}{2} (g_0 \rho^2 + g_1 \mathbf{S}^2)$$

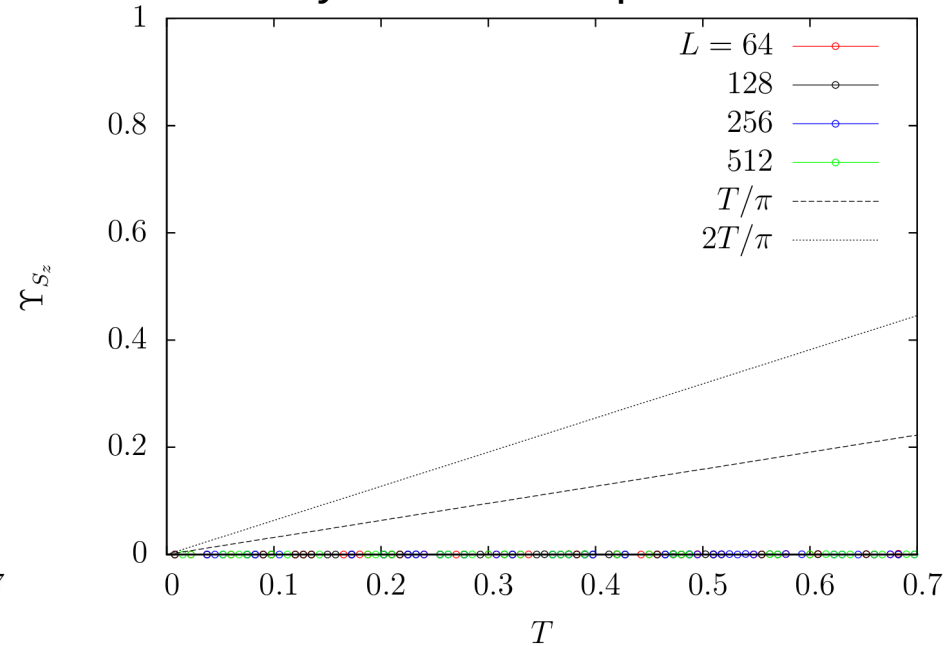


Kosterlitz-Thouless transition in $U(1)$ polar state

Helicity moduls for phase shift



Helicity moduls for spin rotation



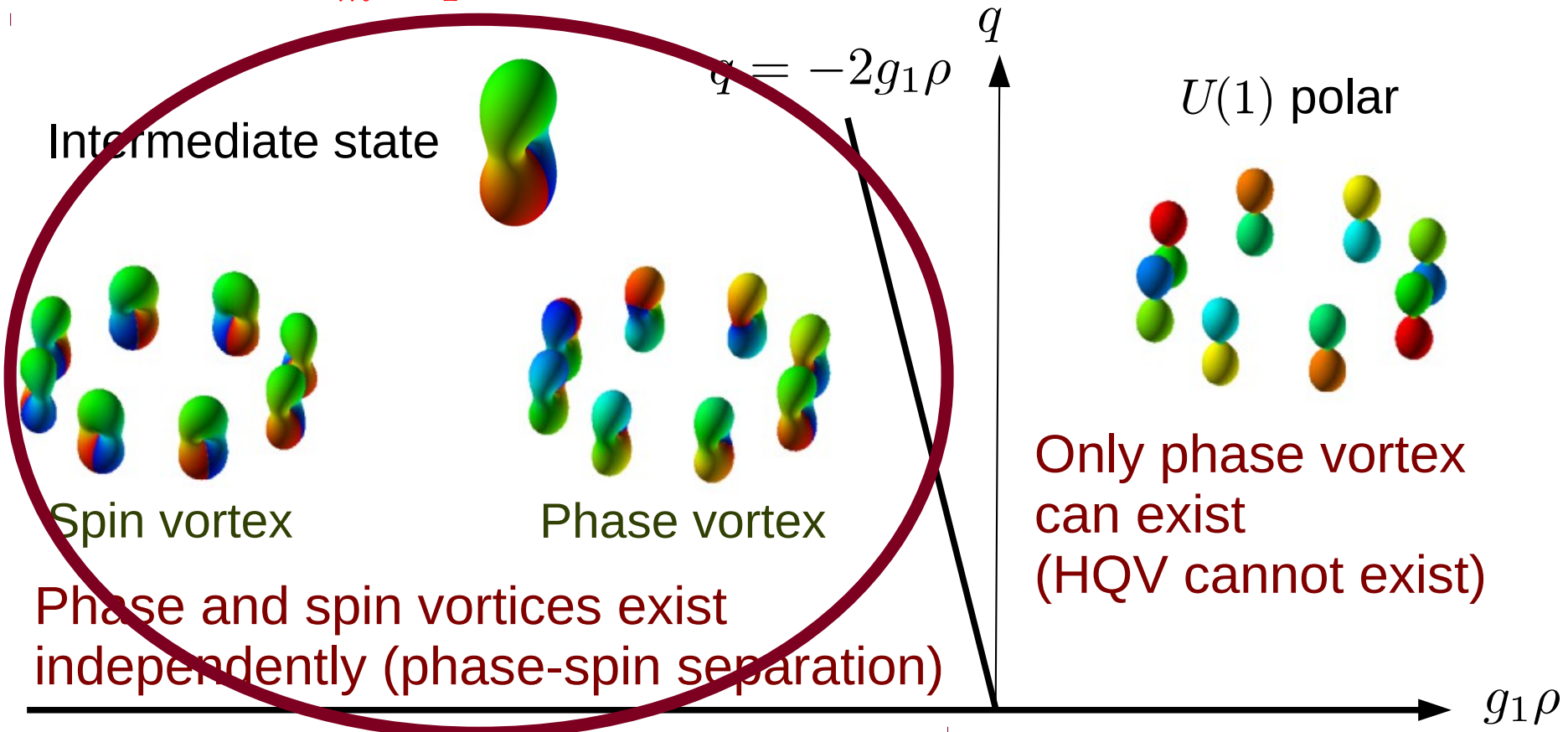
T_{KT} is obtained from Binder cumulant

KT transition is completely same as scale condensate :

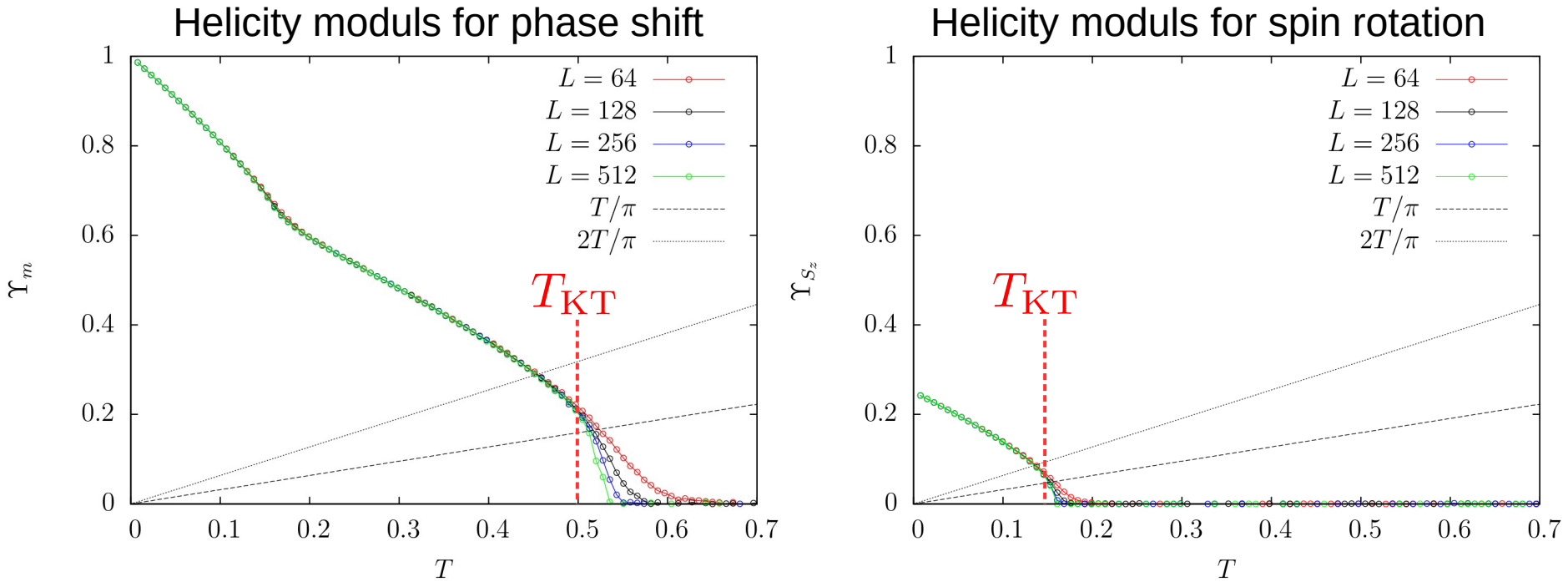
$$\Delta\Upsilon_\phi/T_{KT} \simeq 1/\pi$$

Kosterlitz-Thouless transition in 2D system

$$H = \int d\mathbf{x} \sum_{m=-1}^1 \left(\frac{\hbar^2}{2M} |\nabla \psi_m|^2 + q_2 m^2 |\psi_m|^2 \right) + \frac{1}{2} (g_0 \rho^2 + g_1 \mathbf{S}^2)$$



Kosterlitz-Thouless transition in intermediate state



2-step KT transition occurs at different temperatures for phase shift and spin rotation due to phase-spin separation

Universal jump is the same as that for the scalar condensate :

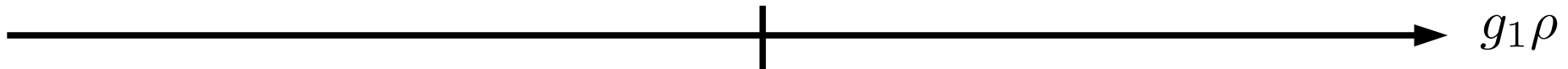
$$\Delta\Upsilon_\phi/T_{KT} \simeq 1/\pi$$

For zero quadratic Zeeman field

$$H = \int d\mathbf{x} \sum_{m=-1}^1 \frac{\hbar^2}{2M} |\nabla \psi_m|^2 + \frac{1}{2} (g_0 \rho^2 + g_1 \mathbf{S}^2)$$

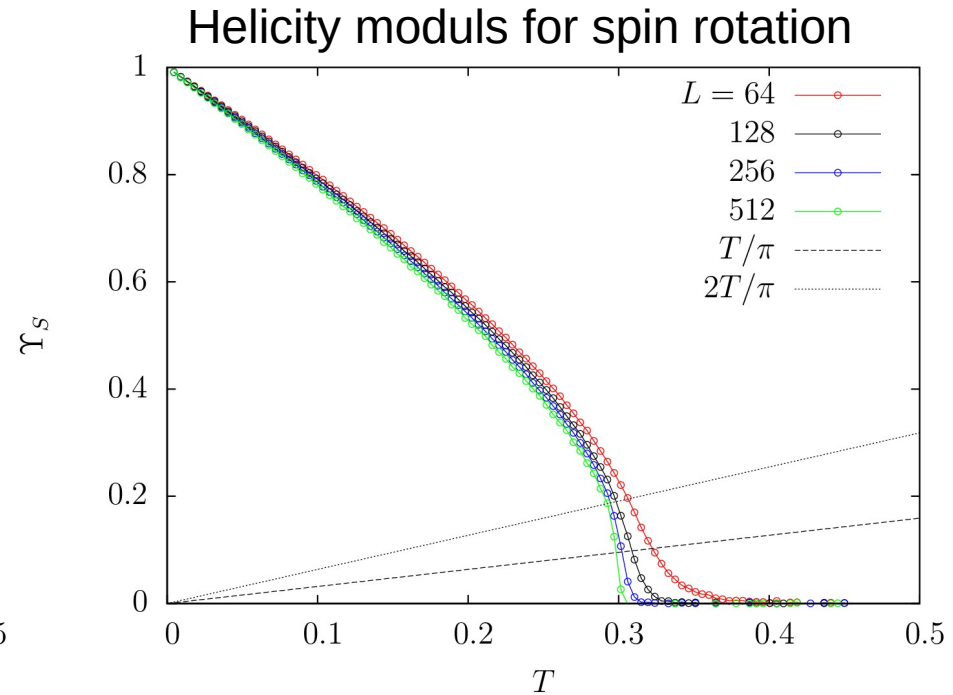
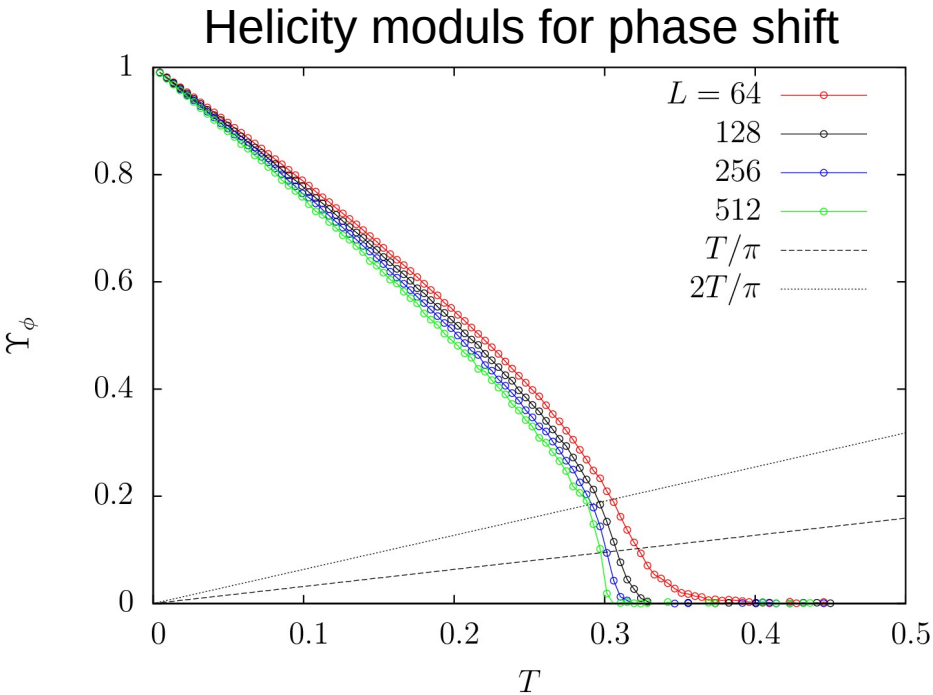
Ferromagnetic : \mathbb{Z}_2 vortex

Polar : half-quantized vortex



Properties of vortices changes discretely between $q > 0$ and $q = 0$

Kosterlitz-Thouless transition in ferromagnetic state

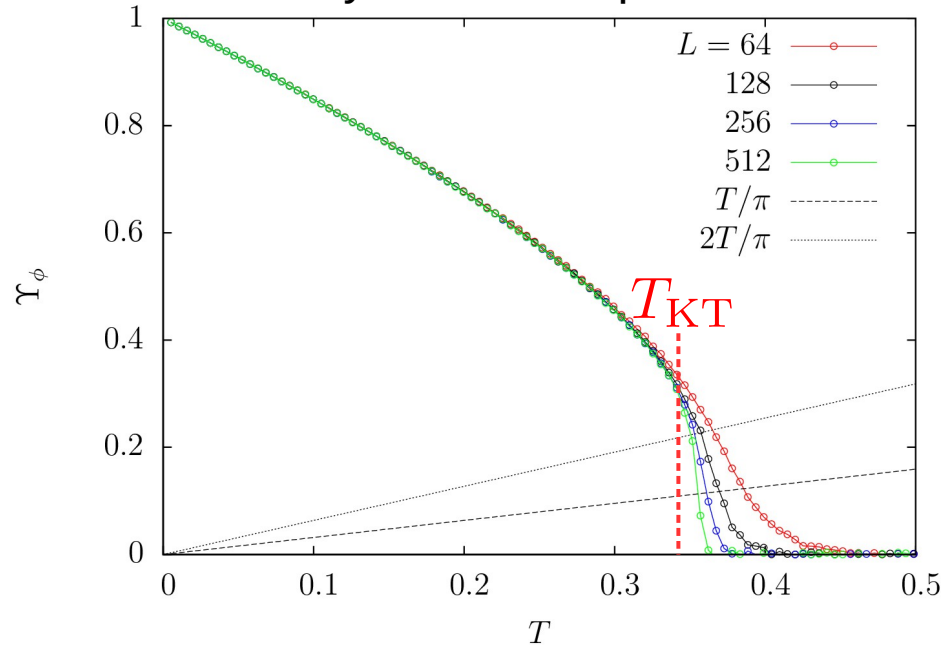


Due to strong finite-size effect, we cannot judge whether KT transition occurs in the thermodynamic limit

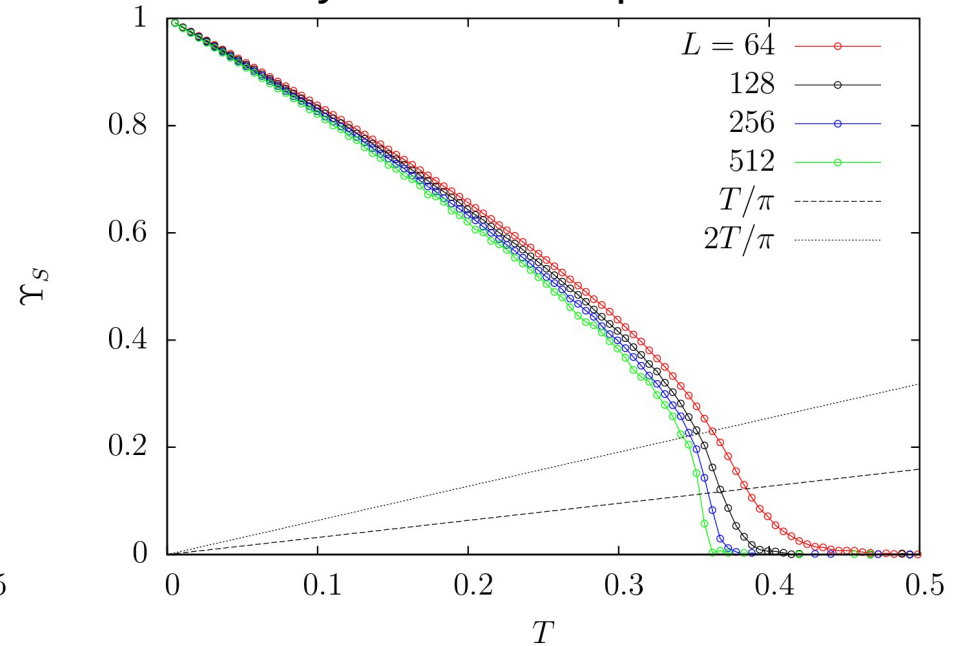
KT transition for \mathbb{Z}_2 vortex has not been solved yet (2D antiferromagnetic Heisenberg model).

Kosterlitz-Thouless transition in polar state

Helicity moduls for phase shift



Helicity moduls for spin rotation

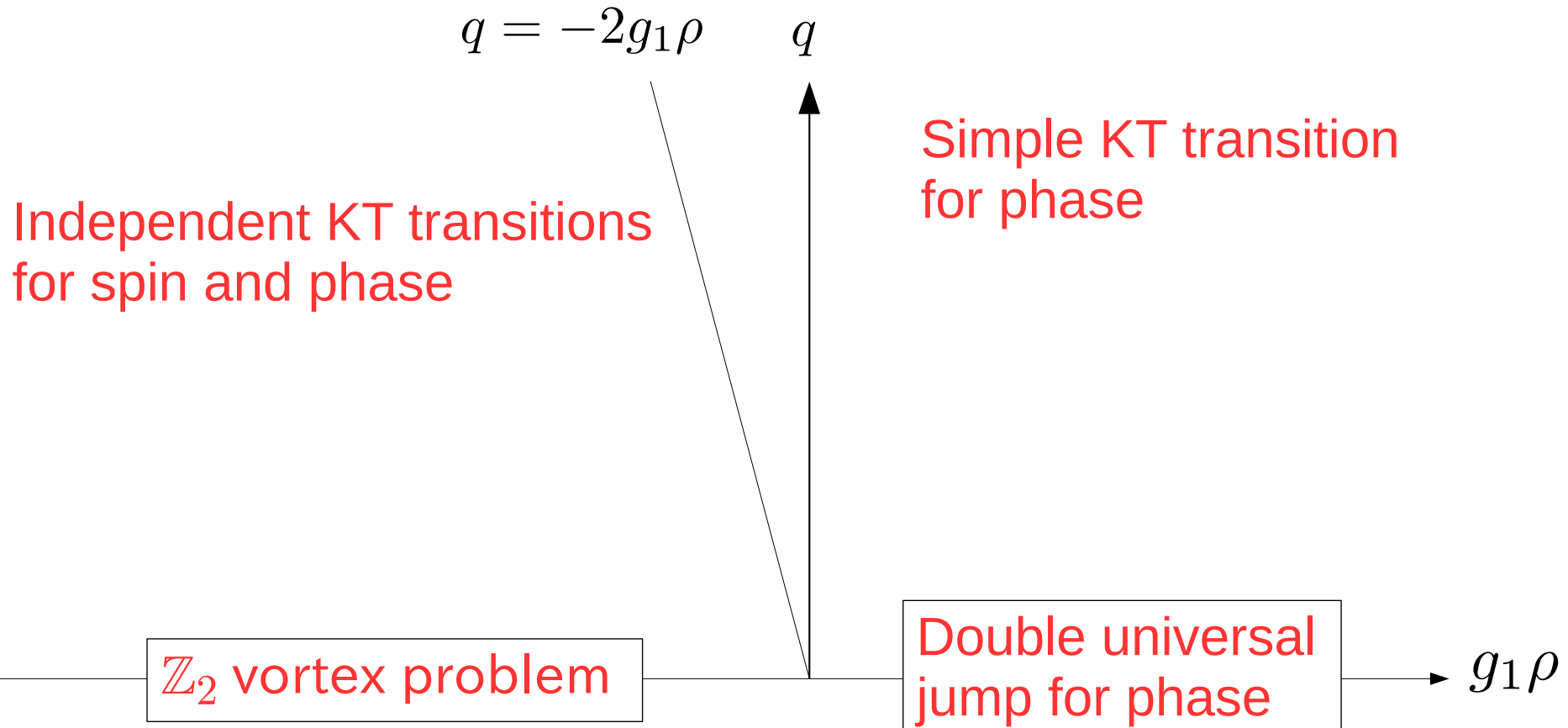


KT transition for phase shift is clear, but that for spin rotation is unclear due to strong finite-size effect (spin part has \mathbb{Z}_2 charge)

Universal jump is 2 times larger than that for the scalar condensate due to half circulation of vortex : $\Delta\Upsilon_\phi/T_{KT} \simeq 2/\pi$

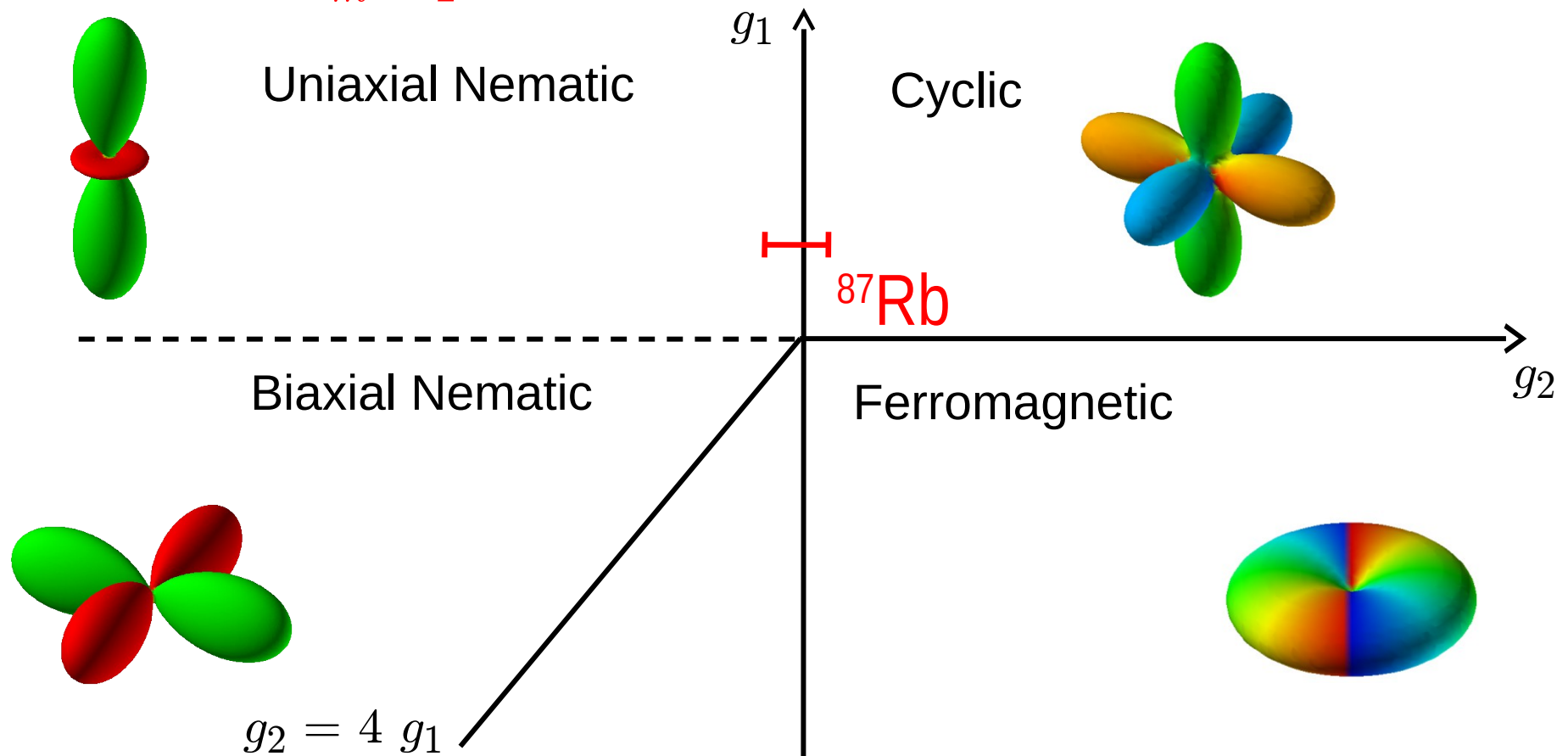
Short summary

Vortex properties can be seen in 2D KT transition

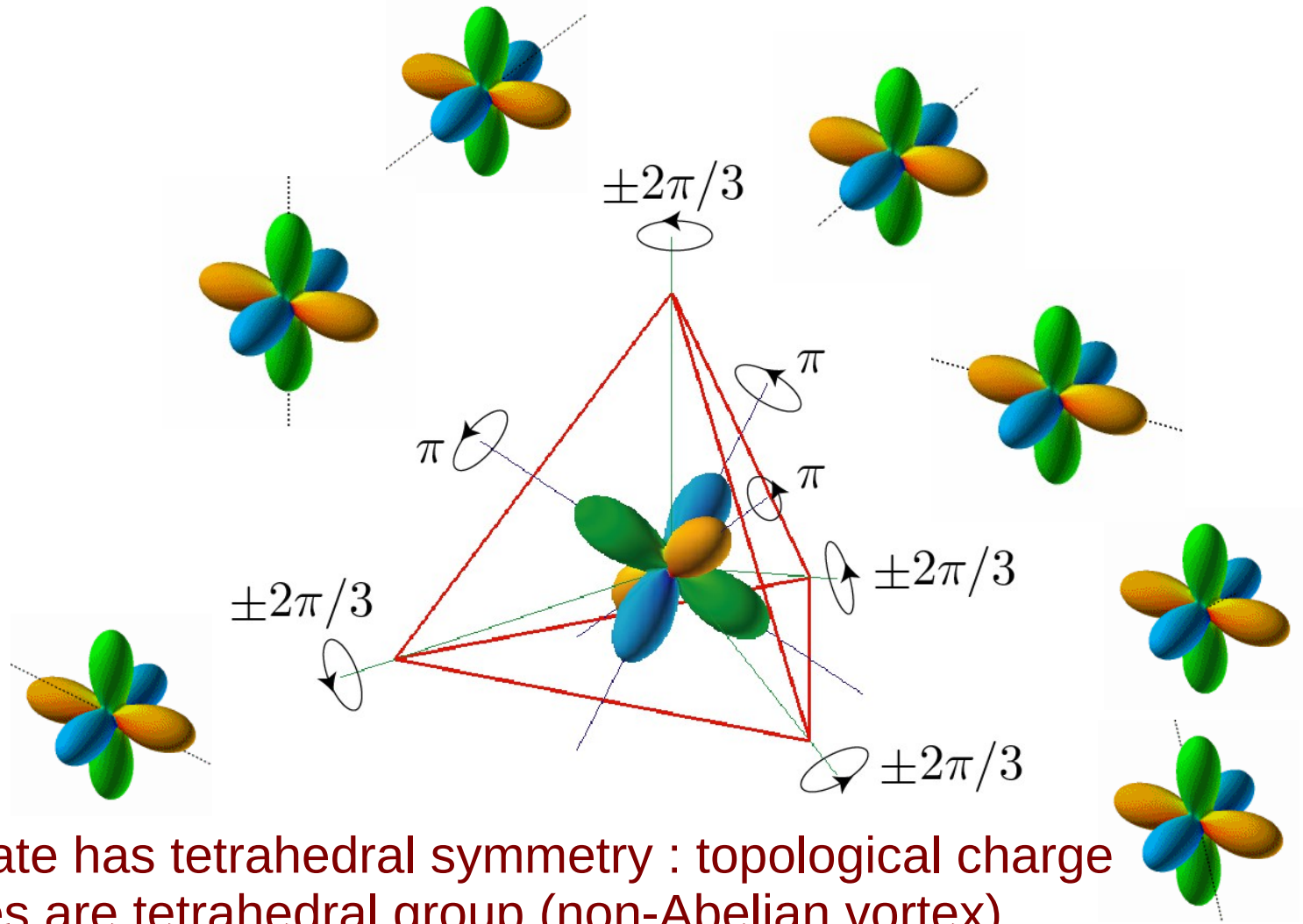


Ground states for spin-2 condensates

$$H = \int d\mathbf{x} \sum_{m=-2}^2 \left(\frac{\hbar^2}{2M} |\nabla \psi_m|^2 \right) + \frac{1}{2} (g_0 \rho^2 + g_1 \mathbf{S}^2 + g_2 |A_{20}|^2)$$



Vortices in cyclic state

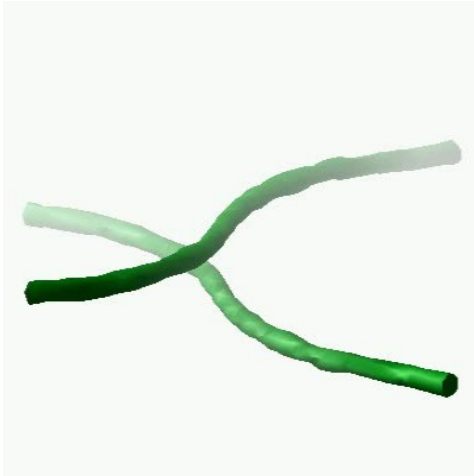


Cyclic state has tetrahedral symmetry : topological charge of vortices are tetrahedral group (non-Abelian vortex)

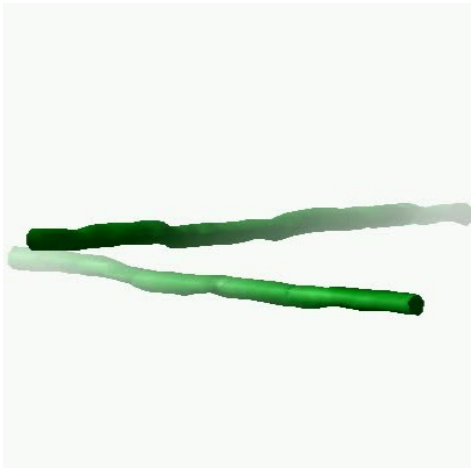
Collision dynamics of vortices

Commutative topological charge

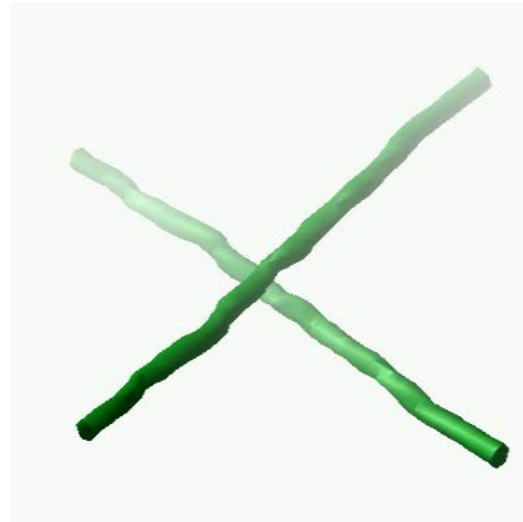
Non-commutative topological charge



reconnection

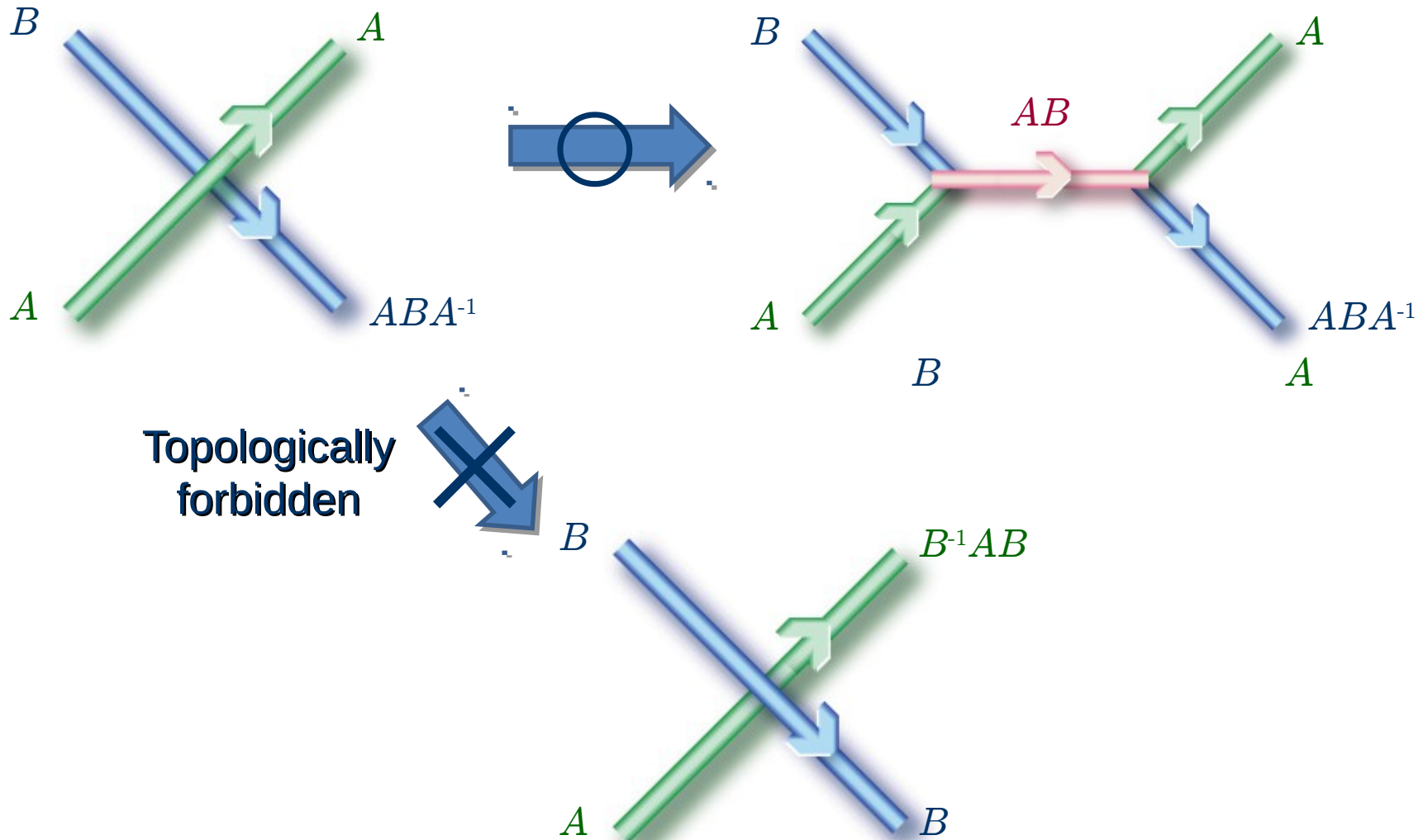


passing through



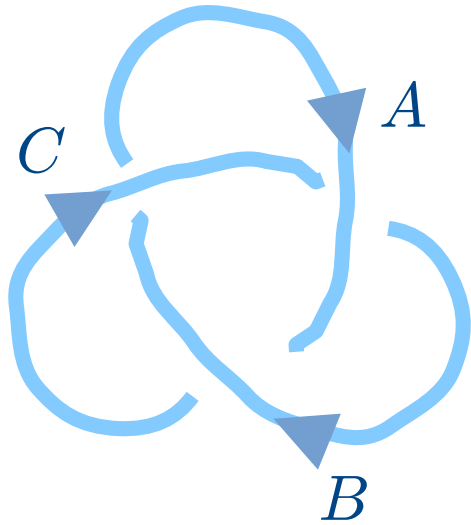
rung

Collision dynamics of vortices



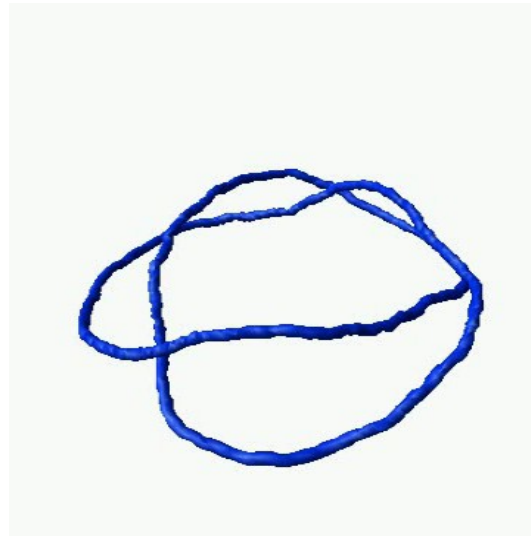
Knots for non-Abelian vortex

Trefoil with orientation
(parity broken)



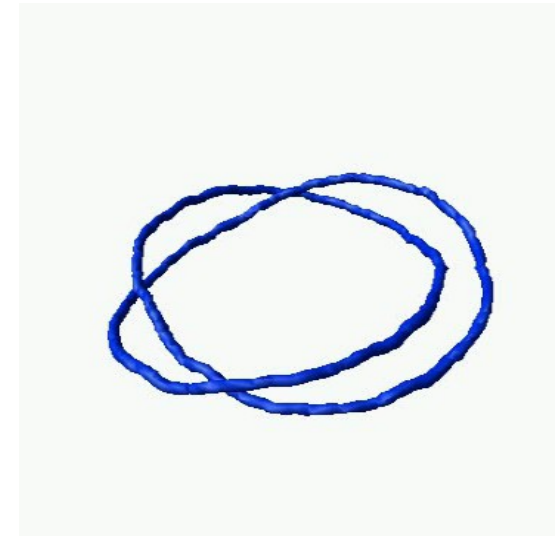
A, B, C are non-commutative

commutative



Knot is unraveled

non-commutative

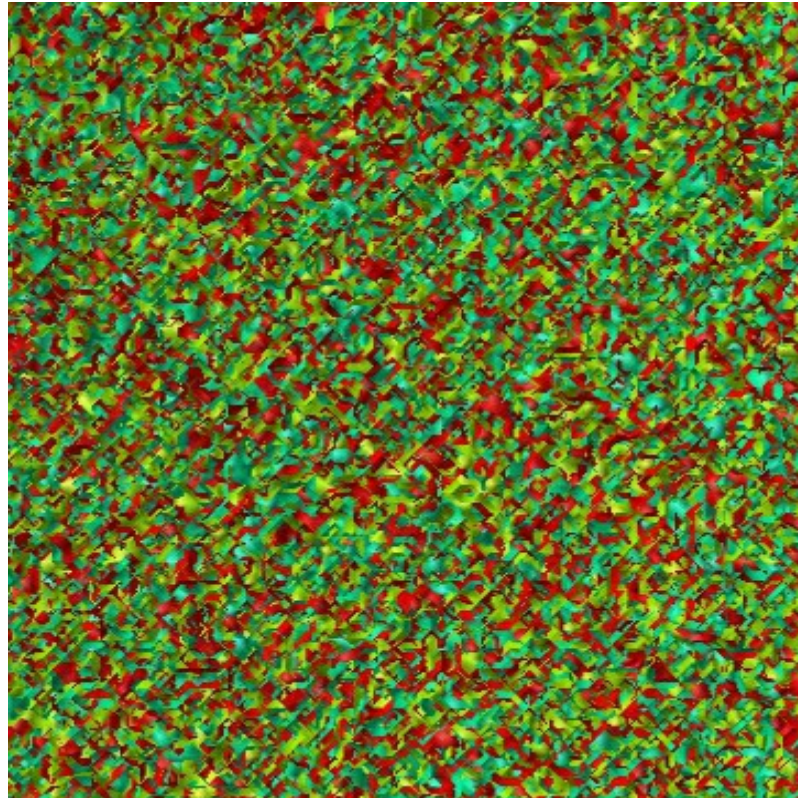


Knot is stable

- New kind of topological structure not classified by Homotopy and not suffered from Derrick's theorem
- Vortex knot breaks chiral symmetry with finite helicity

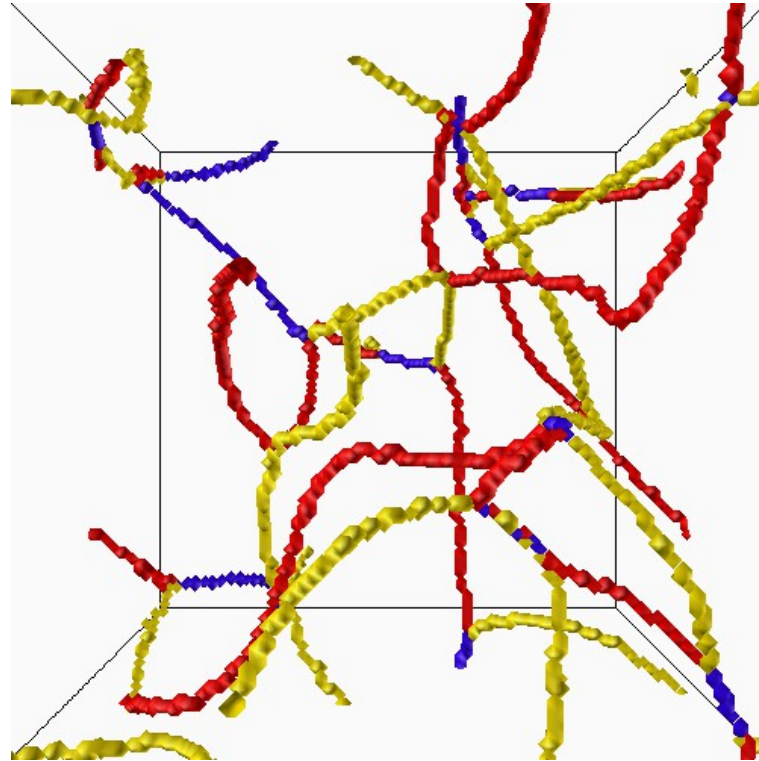
Ordering dynamics after temperature quench

Initial state : fully randomized state surrounded (high temperature) with low-energy uniform ground state (heat reservoir)



Ordering dynamics after temperature quench

Final state



Large scaled knotted vortex structure is remained with finite helicity
→ spontaneous breaking of chiral symmetry with vortex knot

Short Summary

- Vortices becomes non-Abelian for spin-2 spinor condensate (cyclic state)
- Non-Abelian vortices enable new topological defect : vortex knots
- Vortex knots have finite helicity (chirality) and metastable not suffering from Derrick's theorem
- Large scaled vortex knotted structure (chirality) is expected after the temperature quench with spontaneous chiral symmetry breaking

Thank you very much for your attention